The Improvement of Compatibility in Glass Fiber Reinforced PA6/PP Blends

M. B. Andreeva[a]; T. N. Novotortzeva[a]; E. V. Kalugina[a]; V. A. Tochin[a]; L. N. Gurinovich[b]; T. I. Andreeva[b]; I. G. Kalinina[c]; K. Z. Gumargalieva[c]; G. E. Zaikov[d]
[a] Research and Production Company "Polyplastic", [b] Research Institute for Plastics, [c] Institute of Chemical Physics, [d] Institute of Biochemical Physics, Russian Academy of Sciences,

PLEASE SCROLL DOWN FOR ARTICLE

The Improvement of Compatibility in Glass Fiber Reinforced PA6/PP Blends

M. B. ANDREEVA [a], T. N. NOVOTORTZEVA [a], E. V. KALUGINA [a],
V. A. TOCHIN [a], L. N. GURINOVICH [b], T. I. ANDREEVA [b], I. G. KALININA [c],
K. Z. GUMARGALIEVA [c] and G. E. ZAIKOV [d],*

[a] *Research and Production Company "Polyplastic",*
[b] *Research Institute for Plastics,* [c] *Institute of Chemical Physics,*
[d] *Institute of Biochemical Physics, Russian Academy of Sciences*

Rheological properties (melt flow index and melt stability), mechanical properties (tensile strength, flexural strength and impact) of polyamide (PA6) polypropylene (PP) blends were investigated. Influence of potential compatibilizors: 4,4′-diphenylmethane carbodiimide (OCDI), 4,4′-diphenylmethane bismaleimide (BMI) and 2,2′-(1,4-phenylene)-bisoxazoline (OX) on mechanical properties and thermostability of initial and glass reinforced polymer blends was also investigated too. We tried to study the structure of glass fiber reinforced composites by mercury intrusion porosimitry. The influence of compatibilizors on molecular weight of PA6 was studied by GPC, on chemical structure of blends was investigated by NMR and IR-spectroscopy. Addition of OCDI and OX (chain extenders) preserves the product formation as the react with the active and carbonyl groups of PA6. BMI has lower reactivity. Grafting of BMI to PP chains improves compatibility in PA6/PP blend and increases PP adhesion to glass fiber.

Keywords: Rheology; mechanical properties; polyamide (PA6); polypropylene; blends; compatibilizors; structure

INTRODUCTION

The development of polymer blends and alloys is founded upon the thermodynamic theory of mutual solution of polymers and colloid

---

*Corresponding author.

chemistry of dispersion [1]. In terms of modern knowledge, the kinetic stability of polymer blends originates in high viscosity of components, large size of macromolecules and supermolecular formations, low interfacial tension and the existence of transition layers [1, 2]. The structure formed at polymeric material processing determines the properties of the composite [1].

The main problem of the development of polymer blends is compatibility of the components. Good compatibility allows us to obtain homogeneous or heterogeneous melts with good quality and delamination is not displayed after cooling. The methods of compatibility perfection for unfilled PA6/PP blends are reported in [3–5]. As compatibilizors, the authors have used polypropylene modified with maleic anhydride or acrylic acid. At the same time, there are only a few data concerned with reinforced PA/PP blends.

The aim of this study was to improve the compatibility of glass reinforced PA6/PP (80:20) blends with the help of the following additives – oligocarbodiimide (OCDI), bisoxazoline (BOX) and bismaleimide (BMI). We also studied unfilled PA6/PP blends.

MATERIALS AND METHODS

Polyamide PA6, grade 310/210, (Russian Standard 6-06-09-93)
Polypropylene, trade name Lipol
Glass roving, grade RBH 13-2520-76T, (Russian Standard 17139-79)
4,4'-Diphenylmethane carbodiimide (OCDI) – laboratory product, synthesized according to the method [23].

4,4'-Diphenylmethane bismaleimide (BMI) – commercial product (STP 6-05-231-266-86).

2,2'-(1,4-phenylene)-bisoxazoline (OX) – laboratory product with meltting point 240°C.

Composites were prepared by compounding. Double screw extruder was used, $l/d = 25$, 160 – 180 r/min. Processing temperatures 180 – 250°C.

Standard samples for mechanical tests were molded on the Thermoplast-automate Allrouder 221U/150 Arburg Maschinenfabrik Hehl and Sohne. Processing temperatures 220 – 260°C, the temperature of the form 85°C.

Mechanical properties were determined according to Russian Standards:

262-80 – Tensile strength (σ_t)
4648-71 – Flexural strength (σ_f)
4647-80 – Charpy impact strength (a)

Melt flow (*MF*) was evaluated according to Russian Standard 11645-73.

Water absorption (X, %) was evaluated as the changes in the samples weight after 24 hrs in water at room temperature.

TGA, DTA curves were obtained using Simultaneous Thermoanalyser STA 781 (Stanton Redcroft). Test portion 10–20 mg, heating rate 10°/min, in air.

IR-spectra were recorded on IR spectrometer Specord M80 (Karl Zeiss). The films obtained from PA6 solution in formic acid and/or molded films with thickness 15–20 μ were used as test specimens. Assignments of absorption bands were made according to [22].

^{13}C *NMR*-spectra were recorded on NMR spectrometer Gemini-300 (Varian) for PA6 solutions in formic acid-d_2. Assignments for chemical shifts were performed using model compounds and NMR-spectra Catalogs.

GPC High Temperature Chromatograph 150C ALC/GPC (Waters) was used. Detector-refractometer, eluent *m*-cresol, columns with Microgel 10^3, 10^5, PL-gel 10^4. Column temperature 100°C, eluent velocity 1 ml/min, volume for testing 200 ml, concentration 2 mg/ml. Calibration with the help of PS-standards following by Mark-Hauwink correlation for PA6 samples with known molecular weight.

Hg-porosimetry Microporosity of the samples was investigated with porosimeter Autoscan (Autochrom). The volume of mercury forced into the pores at increasing pressure was automatically recorded. The following parameters were calculated from the data obtained:

Total interior pore volume (the volume of mercury forced into the pores at $P = 228$ MPa);
Total pore surface;
Pore surface distribution;

Average, maximal, minimal radius of the pores and the volume, corresponding to each type of pores.

DISCUSSION

Polyolefins have no polar groups in macromolecules and have therefore, only slight adhesion to glass [6]. The same property determines PP and PA incompatibility. The addition of PP to glass reinforced PA6 leads to a significant decrease of mechanical properties (Tab. I). This effect arises from the poor adhesion of PP to PA and PP to glass fibers.

Table II demonstrates the mechanical properties for PA6/PP (80/20) composites, containing optimal concentration of compatibilizors. Modifiers were added at the stage of compounding. Concentrations of potential compatibilizors were chosen according to literature [3 – 5, 7 – 9] and NIIPM specialist's recommendations:

OCDI – 0.5 – 1.0% by weight;
OX – 1.0 – 2.0% by weight
BMI – 0.3 – 1.0% by weight

TABLE I   Mechanical properties of glass reinforced PP, PA6 and PA6/PP

Material	σ_t, MPa	σ_f, MPa	a, kJ/M^2	X, %
PA6 30GF	157	220	56	1.6
PP 30GF	36	53	12	0.1
PA6/PP (90/10)30GF	150	180	44	2.0
PA6/PP (80/20)30GF	114	161	34	2.2
PA6/PP (70/30)30GF	84	125	28	4.3

TABLE II   Influence of modifiers on mechanical properties of glass reinforced PA6/PP

Material	σ_t, MPa	σ_f, MPa	a, kJ/M^2	X, %	$MF_{5'}/MF_{20'}$
PA6/PP (80/20)30GF	114	161	34	2.2	3.9/4.8 = 0.81
PA6/PP (80/20)30GF +0.5% OCDI	126	142	26	2.1	2.2/3.5 = 0.64
PA6/PP (80/20)30GF +2.0%OX	144	212	34	1.9	
PA6/PP (80/20)30GF +0.5%BMI	135	199	44	1.2	2.8/3.1 = 0.9

We can see the different influence of additives on the blend properties. The addition of 0.5% of OCDI does not change the material characteristics; while 1% decreases the tensile strength (the material delaminates). Addition of BMI in concentration of 0.5% and 2% of OX is optimal. Further increases of OX concentration gives no noticeable change in the composite properties.

DSC, electron microscopy, thermomechanic tests are usually used for evaluation of the components compatibility [3-5, 12-14]. We tried to study the structure of glass reinforced composites by mercury intrusion porosimetry. As the density of GF blends depends on mutual adhesion of the components, we assumed that the method should permit us to evaluate the influence of potential compatibilizors on the material structure.

Figure 1 shows the dependence of Hg-intrusion volume and residual mercury content from pores radius. Table III displays the average surface and volume pore radius at Hg intrusion and extrusion, namely, at pressure increasing and releasing.

All samples have a porous structure. Surface pores having radius about 7800 Å were detected, their concentration in initial PA6/PP (80/20) 30GF blend was equal to 6.01 v.%, in the blend with OCDI – 4.19 v.%, with OX – 5.73 v.%, with BMI – 2.8 v.%. Addition of BMI or OX leads to a more compact structure in comparison with the base blend and the blend with OCDI. As noted, PA6/PP(80/20)30GF with OX or BMI shows improved mechanical characteristics (see Tab. II).

It is known that OX and OCDI act as polymer chain extenders. As additives to PET and PA, both compounds react with the active carboxylic end groups [9-11]. Possibly, this mechanism is not valid in our case, because the influence of the additives on the composite properties is different.

By comparing the thermostability of initial and modified blends with PA6 and PP, we notice that OCDI and OX do not influence PP thermostability. But BMI improves PP thermostability. For example, mass loss at 250°C for the base PP and PP with addition of BMI (5% by weight) is 10.0 and 5.4 mass % correspondingly.

All tested compounds effect PA6 thermostability. Data for PA6 modified with OCDI, BMI and OX are presented in Table IV.
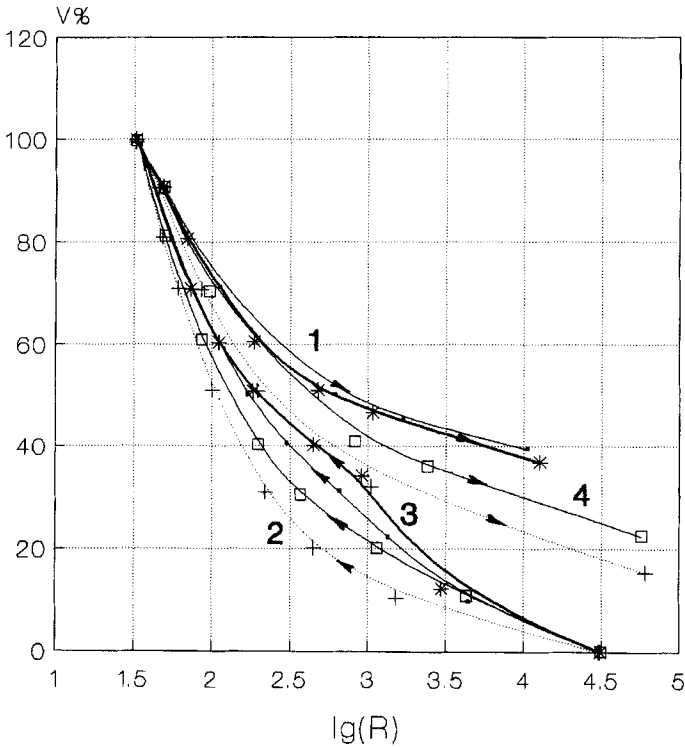
1 – Ny6/PP(80\20)\30GF, 2 – Ny6\PP(80\20)\30GF+0,5(mas)%BMI,
3 – Ny6\PP(80\20)\30GF+0,5(mas)%OCD,4 – Ny6\PP(80\20)\30GF+2,0(mas)%BIS

FIGURE 1   Extrusion and entrusion of pores compositions.

Addition of OCDI complicates processing for the neat PA6 and PA6/PP blends. The greater the OCDI concentration, the greater its the effect.

The influence of OCDI additives on PA6 molecular weight was studied by GPC. Molecular weight characteristics for initial and modified PA6 are presented in Table V. Figure 2 demonstrates chromatograms for initial samples, the samples after compounding and the influence of OCDI in concentration of 0.5 and 1.0 mass %.

A slight decrease of PA6 molecular weight takes place in compounding. OCDI reacts with PA6, as a result polyamide molecular

TABLE III   Pore size and distribution for GR PA6/PP blends

| Sample | Average radius of pores, Å | | | |
| | Hg intrusion | | Hg extrusion | |
	Volume	Surface	Volume	Surface
PA6/PP(80/20) 30GF	1427.0	109.1	3972.0	103.8
PA6/PP(80/20) 30GF + 0.5 mass % OCDI	1285.0	113.2	4568.0	105.8
PA6/PP(80/20) 30GF + 2.0 mass % OX	1328.0	96.55	4761.0	105.8
PA6/PP(80/20) 30GF + 0.5 mass % BMI	732.8	87.7	4950.0	103.6

TABLE IV   TGA and DTA data for unmodified and modified PA6

| Sample | Mass loss, (%) in air, heating rate 10°/min | |
	250°C	300°C
PA6	3.2	4.7
PA6 + 1% OCDI	2.4	4.0
PA6 + 0.5% OCDI	3.0	3.7
PA6 + 1.0% OX	3.1	4.2
PA6 + 2.0% OX	3.5	4.2
PA6 + 0.5% BMI	3.0	4.2

weight significantly increases, and all MMD moments change. M_w doubles with 1.0% of OCDI. As the molecular weight moments show only average numbers, the analysis of chromatographic curve is needed to understand the processes taking place in the polymer.

OX addition in concentration of 0.5–2% does not change PA6 molecular weight (Fig. 2, Tab. V). This phenomenon may be explained by lower reactivity of OX in comparison with OCDI and by lower molecular mass of OX. The alternate explanation is that OX interacts with PA6 end groups. It is known that OCDI participates in branching and crosslinking reactions. Possibly, the branching and crosslinking reactions in glass filled composites proceed more intensely in the

TABLE V   MMD parameters for PA6 modified with OCDI and OX

Sample	M_w	M_n	M_z	M_w/M_n	$[\eta]$
PA6	50000	21000	101000	2.3	0.80
PA6 + 30% GF after extrusion (without additives)	48000	20000	104000	2.3	0.77
PA6 + 30% GF + 0.5% OCDI	68000	26000	167000	2.6	0.99
PA6 + 30% GF + 1.0% OCDI	82000	31000	206000	2.7	1.13
PA6 + 30% GF + 2.0% OX	49000	20000	87000	2.5	0.80
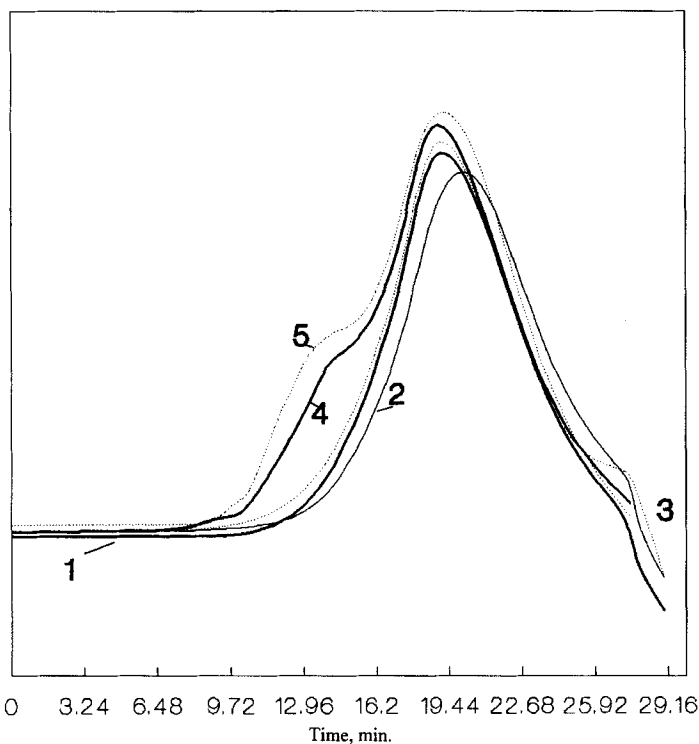
1 – Ny6 – before extrusion, 2 – Ny6\30GF, 3 – Ny6\30GF+2,0(mas)%BIS,
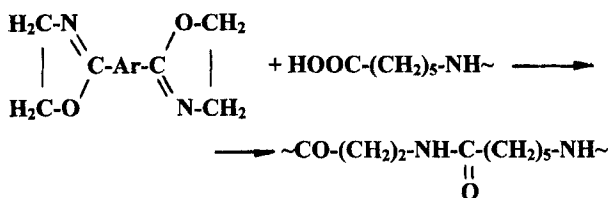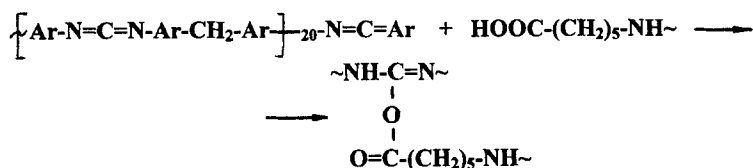4 – Ny6\30GF+0,5(mas)%OCD, 5 - -Ny6\30GF+1,0(mas)%OCD

FIGURE 2   GLC-data for compositions.

presence of OCDI. This is why we were not be able to extrude PA6/PP (80/20)30GF + 1.0% OCDI.

The following scheme describes the reactions between OCDI, OX and PA6 [9 – 11]:

$$\left[Ar\text{-}N=C=N\text{-}Ar\text{-}CH_2\text{-}Ar\right]_{20}\text{-}N=C=Ar \quad + \quad HOOC\text{-}(CH_2)_5\text{-}NH\sim \longrightarrow$$

$$\sim NH\text{-}C=N\sim$$
$$\mid$$
$$\longrightarrow \quad O$$
$$\mid$$
$$O=C\text{-}(CH_2)_5\text{-}NH\sim$$

$$\begin{array}{ccc} H_2C\text{-}N & O\text{-}CH_2 \\ \mid \quad \backslash \quad / \quad \mid & \\ \quad C\text{-}Ar\text{-}C & + HOOC\text{-}(CH_2)_5\text{-}NH\sim \longrightarrow \\ \mid \quad / \quad \backslash \quad \mid & \\ H_2C\text{-}O & N\text{-}CH_2 \end{array}$$

$$\longrightarrow \sim CO\text{-}(CH_2)_2\text{-}NH\text{-}C\text{-}(CH_2)_5\text{-}NH\sim$$
$$\overset{\mid\mid}{O}$$

DTA data (Fig. 3) for the neat PA6/PP blends (PA6/PP ratio 90/10, 80/20, 70/30) and PA6/PP (80/20) + BMI show endothermic peaks at 168, 225°C and an additional endotherm at 204°C. To assign the peak, we separated the blend by the method of sequential extraction. We used formic acid for extraction and obtained several components:
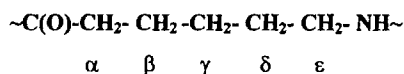
The 1-st and 2-nd extracts have only one DTA peak at 225°C, which may be connected with PA6 melting. PA6 structure is confirmed by IR spectrometry.

The forth extract has DTA peak only at 168°C, corresponding to PP crystallites melting. PP structure is confirmed by IR spectrometry.

The third extract has DTA peak at 204°C. We believe that this product is a result of interactions in PA6/PP melt at processing.

With the help of GPC we studied MMD for the 3-rd extract. As we can see from Table VI, the molecular weight for the product is higher in comparison with PA6.

The structure of the product was also investigated by IR and ^{13}C NMR spectrometry. There are signals of five different CH_2 groups in NMR spectra of the product. The chemical shifts are ≈ 36.7, 26.40, 28.86, 25.70 and 40.18 ppm for α, β, δ, γ, ε C-atoms correspondingly:

$$\sim C(O)\text{-}CH_2\text{-} \ CH_2\text{-}CH_2\text{-} \ CH_2\text{-} \ CH_2\text{-} \ NH\sim$$
$$\quad \alpha \qquad \beta \qquad \gamma \qquad \delta \qquad \varepsilon$$

In spite of the large number of transitions (16000 scans), there is no signal of carbonyl C-atom at 178.93 ppm. In similar conditions
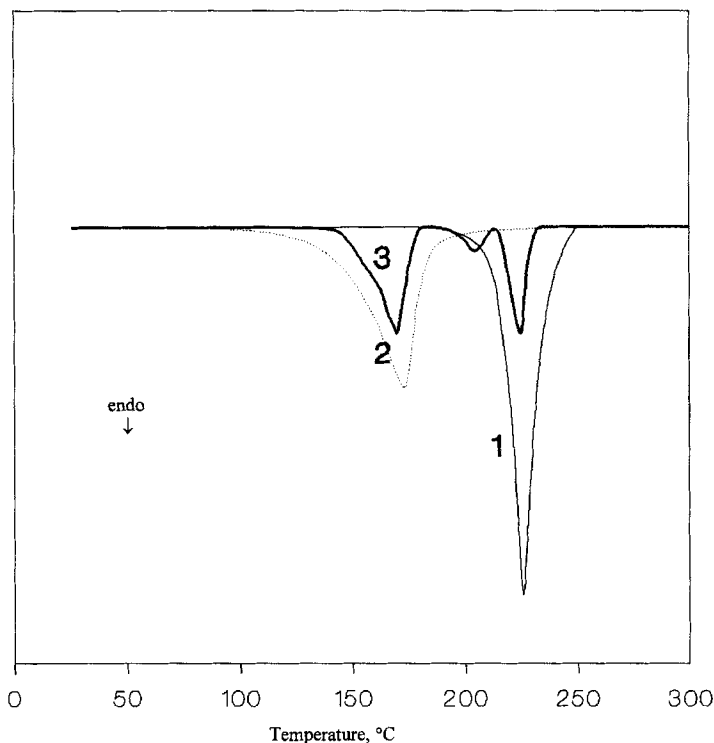
1 – Ny6 , 2 - PP, 3 – Ny6\PP(80\20)\30GF

FIGURE 3   DTA-curves at rate heating 10°/min in air.

TABLE VI   MMD characteristics for PA6 and extracts from PP(80/20)30GF + 0.5% BMI

Sample	M_w	M_n	M_z	M_w/M_n	$[\eta]$
PA6 initial	50000	21000	101000	2.3	0.80
30 GF after extrusion	48000	20000	104000	2.3	0.77
3-rd extract from the composite without additive	56000	20000	107000	2.8	0.87
3-rd extract from the composite with addition of BMI	60000	23000	117000	2.6	0.92

aliphatic PA usually give rather intensive peak in this region. We can notice some broadening and changing of the intensity for the signals of CH_2-group in α-position to carbonyl group (≈ 36.7 ppm). Ordinarily, this signal appears at 37.04 ppm.

The comparison of IR-spectra of the extracted and the neat PA6 showed some differences in the structure. The assignments for the main absorption bands and the ratio of optical densities are tabulated in Table VII. In comparison with PA6, we observe a change of intensities and some signal shifts (as a rule, to ultraviolet area).

The concentration of NCO-groups (Amide 1, Amide 2) relative to aliphatic fragments decreases. Inside the aliphatic fragment the relationship changes too. We interpret the data obtained in the following way: extrusion causes decarboxylation in PA6 and CO_2 evolves. Decarboxylation may proceed with the participation of caprolactam (the possibility of this reaction at 250–290°C was indicated in [15]).

Water absorption tests for standard molded samples (discs, dumbbells) during 160 days showed a progressive chalking. The quantity of a wax product on the material surface increased till 10–12 days. At the same time, a slight shrinkage in the thickness was noticed. We collected the deposit and analyzed it by IR spectrometry. In addition to the main characteristic absorption bands (see Tab. VII), some new absorption bands were found in the spectra of the deposit:

$1680\,CM^{-1}$ – vibrations of C=O groups
$1090\,CM^{-1}$ – ester C—O—C bond
$765\,CM^{-1}$ – aliphatic CH_2 groups
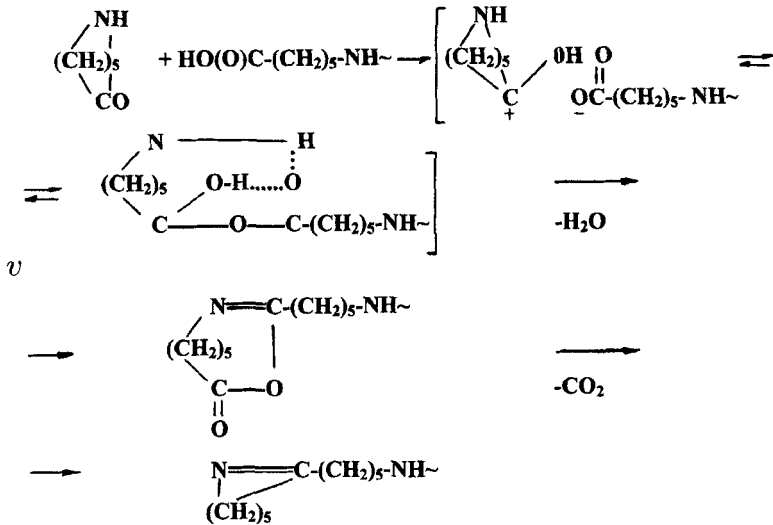$2960\,CM^{-1}$ (unresolved with CM^{-1}) – aliphatic CH_2, CH_3.

The absorption bands confirm the presence of caprolactam moieties in the polymeric chain. This moieties may be associated with the

TABLE VII Assignments for the main absorption bands and optical densities ratio

Vibrations	PA6	Transformation product	Optical densities ratio	PA6	Transformation product
ϑ_{NH}	3324	3300	$D_{NH}/D_{CH_2,CH_3}$	1.41	1.91
ϑ_{NH} (Fermi resonance)	3080	3064	D_{NH}/D_{CH_2}	2.65	2.32
δ_{NCO} (Amide 1)	1648	1638	D_{NCO}/D_{CH_2}	3.26	2.67
$\delta_{NCO, NH}$, ϑ_{CN} (Amide 2)	1568	1546	D_{NCO}/D_{CH_2}	6.12	3.23
δ_{NH}, ϑ_{CN}	1264	1260	D_{NCO}/D_{CH_2}	2.17	1.50
ϑ_{CH_2}	2864	2868	$D_{NY}/D_{CH_2,CH_3}$	4.08	1.81
ϑ_{CH_3}	2948	2948	$D_{CH_2,CH_3}/D_{CH_2}$	1.88	1.21
δ_{NCO}, (Amide 4)	690	692			

following reactions:

$$\underset{\substack{\diagup NH \\ (CH_2)_5 \\ \diagdown CO}}{} + HO(O)C\text{-}(CH_2)_5\text{-}NH\sim \longrightarrow \left[\underset{\substack{\diagup NH \\ (CH_2)_5 \diagup \\ \diagdown C \\ +}}{} \begin{array}{l} OH \ O \\ \ \ \ \ \parallel \\ OC\text{-}(CH_2)_5\text{-}NH\sim \end{array} \right] \rightleftharpoons$$

$$\rightleftharpoons \left[\begin{array}{c} N\text{------------}H \\ \diagup \ \ \ \ \ \ \ \ \vdots \\ (CH_2)_5 \ \ \ \ O\text{-}H......O \\ \diagdown \ \ \ \diagup \\ C\text{------}O\text{---}C\text{-}(CH_2)_5\text{-}NH\sim \end{array} \right] \qquad \longrightarrow \qquad -H_2O$$

v

$$\longrightarrow \quad \begin{array}{c} N\!\!=\!\!\!=\!\!C\text{-}(CH_2)_5\text{-}NH\sim \\ \diagup \qquad \ \ | \\ (CH_2)_5 \qquad | \\ \diagdown \\ C\text{---}O \\ \parallel \\ O \end{array} \qquad \longrightarrow \qquad -CO_2$$

$$\longrightarrow \quad \begin{array}{c} N\!\!=\!\!\!=\!\!C\text{-}(CH_2)_5\text{-}NH\sim \\ | \ \ \ \diagup \\ (CH_2)_5 \end{array}$$

The products with the cyclic end groups, may participate in the reaction with N = C bond rupture. Such reactions lead to branched and crosslinked structures:

As to GPC results, the separated product (especially, extract 3) has higher molecular weight in comparison with the base PA6.

The authors [16, 17] proved that careful purification of PA6 from low molecular fractions noticeably increases the activation energy of decarboxylation. This confirms the significance of low molecular products for the discussed reaction. The reaction is a result of thermal transformations in PA6. In addition we can not exclude the mechano-destruction origin of the product and rheological peculiarities of the blend (PP melt is much more viscous at the processing temperatures). The data for melt flow at 230 and 250°C, presented in Table VIII, support this proposal.

Melt viscosity for PA6 decreases significantly as the temperature increases. Heating in a rheoviscometer channel leads to PA6 destruction and a decrease of the melt viscosity. At real processing conditions an overheating (> 250°C) was noticed that could lead to PA6 destruction.

The investigations allow us to conclude that the third component generated at PA6/PP extrusion does not result from PA6 and PP

TABLE VIII   Effect of temperature and residence time in rheoviscosimeter on PA6 and PP melt flow

Sample	MF_5 at 230°C	MF_{20} at 230°C	MF_5 at 250°C	MF_{20} at 250°C
PP	7.5	5.7	6.9	6.9
PA6	8.2	10.5	15.6	35.3

interaction. The product is formed by thermo- and/or mechano-destruction of PA6 with caprolactam participation. We think the rheological propertied of the blend encourage this product formation.

Addition of OCDI and OX (chain extenders) preserves the product formation as the additives react with the active end carbonyl groups. BMI has lower reactivity, and we observe an additional endotherm peak at 204°C in DTA curve for both the blend with BMI and for initial PA6/PP(80/20) + 30%GF blend. We explain BMI action at processing temperatures by predominant reactions with the active centers in PP and not in PA6 [21]. Such interaction was described in details in [18–20]. Grafting of BMI to PP chains improves compatibility in PA6/PP blend and increases PP adhesion to glass fiber. As a consequence, more dense structure forms, and the mechanical properties of the material are enhanced. Similar effect we can see using PP with grafted BMI groups as a compatibilizor. For example, σ_t and σ_f for the composite PA6/PP + PP5%BMI (80/15 + 5)30%GF are equal 163 и 191 MPa correspondingly.

Acknowledgments

References

[1] Kulesnev, V. N. (1984). Polymer blends M. Znanie, p. 304.
[2] Polymer blends (1981). Edited by Pole, D., Newman, S. and Mir, M.
[3] Lin, J. S., Eric Y. Sheu and Jois, Y. H. R. (1995). J. Appl. Pol. Sci., 55, 655.
[4] Benderly, D., Siegmann, A. and Narkis, M. (1996). Pol. Composites, 17(3), 343.
[5] La Mantia, F. P., Advances in Polymer Technology, 12(1), 47.
[6] Gorbatkina, Ju. A. (1987). Adhesive Strength in Filled Polymer, Chimia, M. (Ed.), p. 191.

[7] C & EN, January 15 (1996), p. 21.
[8] Karitchev, I. A., Bratchikov, A. V. and Budnitzky, Ju. M. (1992). *Plast. Massy*, 6, p. 48.
[9] Krasnov, A. P. (1994). *Visokomolekul. soedin.*, **27**, 126.
[10] Modifizierte Polyamides – neve Moglichkelten (1995). *De Wergill Kunstoffe*, **85**(6), 110.
[11] Lum, R. M. Ed. (1979). *J. Pol. Sci.*, *Pol. Chem.*, **17**(9), 3017.
[12] La Mantia, F. P. and Valenza, A. (1988). *Eur. Polym. J.*, 9, p. 825.
[13] Sachin N., Sathe, Surekha Devi, Srinivasa Rao, G. S. and Rao, K. V. (1996). *J. Appl. Pol. Sci.*, **61**, 97.
[14] Gonzalez-Monteil, A., Keskkula, H. and Paul, D. R. (1995). *J. Pol. Sci.*, Part B, *Pol. Physics*, **33**, 1751.
[15] Reimschuessel, H. K. and Dege, G. J. (1970). *J. Polym. Sci.*, A1, **8**, 3265.
[16] Straus, S. and Wall, L. (1958). *Res. Nat. Bur. Stand.*, **60**, 35.
[17] Straus, S. and Wall, L. (1959). *Research*, **63A**, 269.
[18] Dagli, S. S., Xanthos, M. and Biesfinberger, J. A. (1994). *Polym. Eng. Sci.*, **34**(22), 25.
[19] We, S. (1987). *Polym. Eng. Sci.*, **27**(22), 335.
[20] Aji, Abdellah and Utracki, L. A. (1996). *Polym. Eng. and Sci.*, **36**(12), 1574.
[21] Vinogradova, G. V. and Malkin, A. J. (1977). *Peology of Polymers*, Chimia, M. (Ed.), p. 438.
[22] Infrared Spectroscopy of Polymers, (1976). Edited by Oleynik, E. Ph. Chimia, M. (Ed.), p. 472.
[23] *J. Polymer Sci.*, *Polymer Symp.*, 1978, **62**, 309.